pEGFP-N1介导BTI的表达抑制肝癌HepG2细胞迁移及细胞周期进程

李玉英[1]* 白崇智[2]

([1]化学生物学与分子工程教育部重点实验室, 山西大学生物技术研究所, 太原 030006;
[2]山西省中医药研究院, 太原 030012)

摘要 荞麦是一种药食同源的粮食作物, 研究发现荞麦胰蛋白酶抑制剂(BTI)可以抑制肿瘤细胞的增殖。该文采用激光共聚焦显微镜、MTT法、划痕法、流式细胞术、qRT-PCR、Western blot等方法检测了pEGFP-N1介导的BTI在HepG2细胞内的表达对细胞的生长、黏附、迁移、凋亡及细胞周期的作用。结果显示, pEGFP-N1介导的BTI在HepG2细胞内的表达显著抑制了细胞生长、黏附和迁移, 并使HepG2细胞凋亡率增加。同时E-钙黏蛋白的表达水平增高, MMP-2和MMP-9的表达下降。伴随着p53、p21、p63、p73的上调表达, 周期蛋白CyclinD1、CyclinE1和周期依赖性激酶(CDK2、CDK4、CDK7)的表达下调, 细胞周期阻滞在G_1期。

关键词 荞麦胰蛋白酶抑制剂(BTI); 肝癌; 细胞周期; 迁移; p53; 基质金属蛋白酶

pEGFP-N1-Mediated BTI Expression Inhibits Migration and Cell Cycle Progression in Hepatocellular Carcinoma HepG2 Cells

LI Yuying[1]*, BAI Chongzhi[2]

([1]*Key Laboratory of Chemical Biology and Molecular Engineering of the Ministry of Education, Institute of Biotechnology, Shanxi University, Taiyuan 030006, China*; [2]*Chinese Medicine Hospital of Shanxi Province, Taiyuan 030012, China*)

Abstract Buckwheat, a specialty grain in China, is a common component of food products and medicines. BTI (Buckwheat trypsin inhibitor) reportedly inhibits tumor cells growth. Laser confocal microscopy, MTT assay, wound healing assay, flow cytometry, qRT-PCR, and Western blot were used to investigate the effect of cell viability, adhesion, migration, apoptosis, and cell cycle after pEGFP-N1-BTI transfected in human hepatocellular carcinoma HepG2 cells. The pEGFP-N1-mediated BTI expression significantly inhibited proliferation, adhesion, and migration of HepG2 cells. Meanwhile, the cell apoptosis rates were increased and the cell cycle was arrested. Moreover, pEGFP-N1-mediated BTI enhanced the protein expression level of E-cadherin and decreased those of MMP-2 and MMP-9. The potential mechanism involved the following: p53, p21, p63, and p73 up-regulation; CyclinD1, CyclinE1, and cyclin-dependent kinases (CDK2, CDK4, and CDK7) down-regulation; and arrest of the HepG2 cells cycle in G_1 phase.

Keywords BTI (Buckwheat trypsin inhibitor); hepatocellular carcinoma; cell cycle; migration; p53; matrix metalloproteinase

收稿日期: 2020-06-16 接受日期: 2020-08-03
山西省重点研发计划(批准号: 201903D321095)和山西省高等学校科技成果转化培育项目(批准号: TSTAP 2019-6)资助的课题
*通讯作者。Tel: 0351-7011499, E-mail: lyy9030@sxu.edu.cn
Received: June 16, 2020 Accepted: August 3, 2020
This work was supported by Key Projects of Shanxi Province (Grant No.201903D321095) and the Foundation of Transformation of Scientific and Technological Achievements Programs of Higher Education Institutions in Shanxi (Grant No.TSTAP 2019-6)
*Corresponding author. Tel: +86-351-7011499, E-mail: lyy9030@sxu.edu.cn
URL: http://www.cjcb.org/arts.asp?id=5356

HCC (hepatocellular carcinoma) is a malignant tumor with high incidence, difficult treatment, and high mortality. Despite recent advances in diagnostic modalities, the limited treatment remedies for HCC and the poor prognosis emphasize the importance of developing an effective treatment for this disease[1]. In anticancer drug research, trypsin inhibitors in organisms are found to combine with corresponding proteases through various pathways to inhibit the proliferation, invasion, and migration of tumor cells, thereby providing new ideas for the development of anticancer drugs[2].

TI (trypsin inhibitor) belongs to the serine protease inhibitor family that can inhibit various proteases, such as trypsin, thrombin, and lysosomal enzymes. TIs have good antibacterial and anti-insect properties. It is effective for the treatment of HIV and diabetes. Meanwhile, TIs help preventing and treating cerebral ischemia[3-4]. The antitumor activity of TI is interesting. BBIs (Bowman-Birk inhibitors) derived from the soybean are particularly effective in suppressing carcinogenesis[5]. The BBI concentrate is a promising tumor-preventive agent. In recent years, another inhibitor identified from buckwheat and belonging to the potato I-type family has become the focus of research attention. Buckwheat is an ancient and specialty grain in China. Buckwheat has many uses in food and medicine due to its unique chemical and bioactive components. Several TIs from buckwheat seeds have been reported, including BWI-1, which can inhibit T-acute lymphoblastic leukemia cells[6].

We find a recombinant BTI that can inhibit the growth of IM-9 cells and MCF-7 cells *in vitro* and induce the apoptosis of tumor cells[7-8]. Notably, it has no effect on normal human peripheral blood mononuclear cells. The mechanism and effect of BTI on cell migration and cell cycle progression in tumor cells are poorly understood.

GFP reporter gene, as a marker used for screening living cells in tumor gene therapy, provides a simple observation method. This approach is convenient and time-saving, with no toxic side effects. It has been widely used in research works on gene expression regulation, transgenic animals, protein localization in cells, and migration change.

In this study, we constructed the eukaryotic expression plasmid pEGFP-N1-BTI and performed the liposome-mediated transfection of HepG2 cells. Laser confocal microscopy was used to observe fusion gene expression in cells. Furthermore, we investigated the underlying molecular mechanisms and effects of pEGFP-N1-BTI on the migration and cell cycle progression of HepG2 cells. This study aimed to assess the antitumor efficacy of BTI gene therapy and to develop a new therapeutic strategy for HCC.

1 Materials and Methods

1.1 Reagents, antibodies and cells

MTT [3-(4,5-dimethylthiazol-2-yl)-2,5-diphenyltetrazolium bromide] was purchased from Sigma. pEGFP-N1 was obtained from Clontech. Lipofectamine™ 2000 was purchased from Invitrogen. ECL (enhanced chemiluminescence) kit was purchased from Engreen Biosystem in China. pGEM-T easy vector was purchased from Promega. Annexin V-FITC apoptosis detection kit was obtained from Pharmingen–Becton Dickinson in USA. BCA Protein Assay Kit was purchased from Beyotime Institute of Biotechnology in China. Total RNA isolation kit was purchased from TaKaRa Biotechnology. SYBR Premix Ex Taq™ was purchased from QIAGEN. Antibodies against p53, p63, p73, p21, cyclinD1, CDK2, CDK4, CDK7, E-cadherin, MMP-2, and MMP-9 were purchased from Santa Cruz.

The human hepatocellular carcinoma cell line HepG2, human normal liver cell line HL-7702 were obtained from the Institute of Cell Research (Shanghai, China). Cells were cultured in DMEM medium (Gibco, USA) containing 10% (*v/v*) fetal calf serum (Hangzhou Sijiqing, China), 100 U/mL penicillin, and 100 μg/mL streptomycin at 37 °C and in a humidified 5% CO_2 atmosphere.

1.2 Construction of plasmids and transfection

The sequence of *BTI* gene was cloned from buckwheat by PCR amplification, ligated into the pGEM-T

easy vector, and then subcloned between the *Hin*d III/*Bam* HI sites of eukaryotic expression vector pEGFP-N1 (EGFP) to construct the recombinant plasmid pEGFP-N1-BTI (BTI-EGFP). HepG2 cells (2×10^4 cells/well) in a 24-well plate were transiently transfected with Lipofectamine™ 2000.

Cells were incubated with 1.0 μg plasmid DNA (pEGFP-N1 and pEGFP-N1-BTI) and 2.5 μL of Lipofectamine 2000 at room temperature for 5 min. After 48 h, the cell culture medium was aspirated. Cells were washed with PBS (phosphate-buffered saline) twice and then fixed with a fixative (70% ethanol formulation, 4% formaldehyde, and 5% acetic acid) for 5 min. Cells were washed thrice with PBS to remove the fixative. Then, the transfection efficiency was monitored by using green fluorescent protein with a FV1000 laser scanning confocal microscope (Olympus, Tokyo, Japan). The expression of BTI in cells was further confirmed by Western blot analysis using BTI antibody.

1.3 Cell viability assay

To evaluate the cytotoxic effect of BTI, cell viability was determined by MTT assay. Cells were transfected with plasmid DNA (pEGFP-N1-BTI) or control plasmid pEGFP-N1 for 48 h. After treatment, MTT (5 mg/mL) was added and incubated for 4 h. Following this reaction, the medium was removed, and 150 μL of DMSO was added to dissolve the purple dye. The absorbance at 570 nm was measured using a microtiter plate reader (Bio-Rad model 550). Cell viability was assessed based on D_{570} Experiment group/D_{570} Control group×100%.

1.4 Morphological observation

HepG2 cells were planted into 6-well plates and allowed to attach for 24 h before treatment. Then, the cells were transfected with plasmid DNA. After treatment, cells were re-suspended in the fixation solution (4% paraformaldehyde) for about 10 min and then stained with DAPI (2 μg/mL) for 5 min. The cell nuclear morphology was observed by a laser confocal microscope. Apoptotic cells were evaluated by their nuclear fragmentation and condensation.

1.5 Flow cytometric analysis

Flow cytometric analysis of apoptosis cells was performed using an apoptosis detection kit. The cells were re-suspended in 500 μL of binding buffer, containing 5 μL of fluorescence-conjugated Annexin V-FITC and PI. The suspension was then incubated for 30 min in the dark. Afterward, the cells were detected using flow cytometry (FACSCalibur, BD, USA). Data analysis was performed using Cell Quest software (Becton Dickinson, San Jose, USA)[8].

Cell cycle analysis: the cells were fixed in 70% cold ethanol, washed with PBS, and then stained with PI (1 mmol/L) and RNase A (1 mmol/L) in PBS for 30 min in the dark. Cell distribution in the different phases of the cell cycle was detected by flow cytometry using the ModFit LT V3.0 software (Verity Software House, Topsham, USA)[8].

1.6 Cell adhesion assay

HepG2 cells (2×10^4 cells/well) were seeded into 96-well plates coated with gelatin and incubated at 37 °C in 5% CO_2 for 1, 2, 3, and 4 h, respectively. The unattached cells were removed by washing with PBS, and the adherent cells were fixed in 4% paraformaldehyde solution. Fixed cells were stained with crystal violet and then solubilized with 1% SDS. D_{570} was measured using a microplate reader. Results were expressed as the percentage of total cells, assuming that the adhesion of cells in the control was 100%. All experiments were carried out in triplicate, and three independent assays were conducted.

1.7 Wound healing assay

The effects of EGFP and EGFP-BTI on HepG2 cells migration were tested using *in vitro* wound healing assay. HepG2 cells were seeded into 24-well plates and grown to form a confluent monolayer. After transfection with recombinant plasmids for 48 h, straight-line scratch wounds were made on the monolayer with a sterile pipette tip. Cells were washed twice with PBS and then incubated in DMEM with 1% serum for 1 day to exclude the effect of the serum on cell growth. Photographs were taken at the indicated time points. The percentage of migration rate was evaluated by compar-

表1 荧光定量PCR所使用的引物

Table 1 Primers used for qRT-PCR

基因 Gene	正向引物(5′→3′) Forward primer (5′→3′)	反向引物(5′→3′) Reverse primer (5′→3′)
GADPH	CCC ATG TTT GTT GTT GGT GTC	TCG TAC CAT GAC TCA AGC TTG
p21	TTG ATTA GCA GCG GAA CA	TAC AGT CTA GGT GGA GAA ACG
p53	GCG CAC AGA GGA AGA GAA TC	GGC CAA CTT GTT CAG TGG AG
CyclinD1	CTG GAT GCT GGA GGT CTG CGA GGA	CTG GCA TTT TGG AGA GGA AGT GTT
CyclinE1	CGT TGC TTC ACT TCT CCT	GAA GGG CTT CAA CTG TTC C
CDK2	ATC CGC CTG GAC ACT GAG	TCC GCT TGT TAG GGT CGT
CDK7	CAC CAT CAC ACA TCA AAG CC	GCC ACT GTT CCT CAG TTG GT

ing the scratch gap among the indicated time points.

1.8 RNA isolation and qRT-PCR

Total RNA was extracted from the cells using RNA isolation kit. Reverse transcription reaction was performed using oligo (dT) and AMV-RT reverse transcription enzyme (5 U/μL). qRT-PCR amplification and detection were performed using the SYBR Premix Ex Taq™. The primer sequences are shown in the Table 1.

qRT-PCR reaction was performed at 95 °C for 4 min (denaturation), followed by 40 cycles at 94 °C for 10 s, 55 °C for 30 s, 72 °C for 60 s, and finally, 72 °C for 5 min. *GADPH* was used as the reference gene, and the relative expression levels of the target genes were measured by the $2^{-\Delta\Delta Ct}$ method.

1.9 Western blot analysis

The whole-cell extract was lysed in cold RIPA extraction buffer (1 mmol/L PMSF, 0.5% deoxycholic acid sodium salt, 0.1% SDS, 1% Triton X-100, 1% aprotinin, and 1% leupeptin) for 30 min on ice. The lysates were centrifuged at 12 000 r/min for 15 min at 4 °C, and the supernatants were collected. Protein concentrations were measured by the BCA protein assay kit. Proteins were separated by 10% SDS polyacrylamide gel electrophoresis and transferred onto a PVDF membrane. After blocking with 5% non-fat milk in Tween-20 (TBST, 0.1%) at room temperature for 2 h, the membranes were incubated overnight with the primary antibody at 4 °C and washed five times with Tris-buffered saline containing 0.05% TBST. Then, the membranes were incubated with the horseradish peroxidase-conjugated secondary antibodies for 1 h at room temperature. The membranes were washed thrice in TBST, after which they were incubated in an enhanced chemiluminescence detection system and exposed to an X-ray film.

1.10 Statistical analysis

Data were presented as the $\bar{x}\pm s$. Statistical analysis was carried out by ANOVA followed by a Dunnett *t*-test. The *P*-values of less than 0.05 ($P<0.05$) and 0.01 ($P<0.01$) indicated that the difference was significant and extremely significant, respectively, compared with the control. All the figures shown in this article were obtained from at least three independent experiments.

2 Results

2.1 HepG2 cells by pEGFP-N1-BTI transfected inhibits cell viability

When HepG2 cells were transfected with pEGFP-N1 and pEGFP-N1-BTI, the BTI-EGFP protein expression was directly examined under the laser confocal microscope and further confirmed by Western blot. Anti-BTI antibody was used to detect the BTI protein. As shown in Fig.1A, the EGFP protein was highly expressed in the HepG2 cells. It showed strong green fluorescence and was evenly distributed throughout the cells when transfected with the EGFP control. The green fluorescence was mostly located in the nucleus, and only a small amount was distributed in the cytoplasm of cells transfected with pEGFP-N1-BTI. The expression of BTI-GFP protein was detected as expected, whereas no signal was detected in the EGFP control when the anti-BTI antibody was used for detection (Fig.1B). These results indicated that the BTI-EGFP protein was expressed in HepG2 cells.

Meanwhile, morphological changes of HepG2

cells were observed by using an inverted microscope. As shown in Fig.1C, the cell body had an irregular shape and large size when transfected with EGFP control. Meanwhile, the HepG2 cells showed significant changes in morphology, as follows: sparse growth, disordered arrangement, uneven size, condensed cytoplasm, and the morphological characteristics of apoptotic cells when transfected with pEGFP-N1-BTI.

Furthermore, the MTT assay was used to detect the cell viability when the HepG2 cells were transfected with pEGFP-N1-BTI. The results presented in Fig.1D indicated that BTI-EGFP could inhibit HepG2 cells proliferation in a time-dependent manner. When the cells were transfected with BTI-EGFP for 12 h, the inhibition rate showed almost no change. At 48 h after transfection, the inhibition rate reached approximately 35%. In addition, the MTT assay was also used to detect the effects of BTI on the viability of HepG2 cells and normal human liver HL7702 cells. After cells were incubated with BTI for 48 h at 37 °C, the absorbance was measured using a microtiter plate reader at 570 nm. As shown in Fig.1E, BTI inhibited the survival of HepG2 cells in a dose-dependent manner, and the inhibitory effects showed statistical significance in the range of 1.25-10 μmol/L (P<0.01), but minimal effects were observed on the normal human liver 7702 cells' rate of

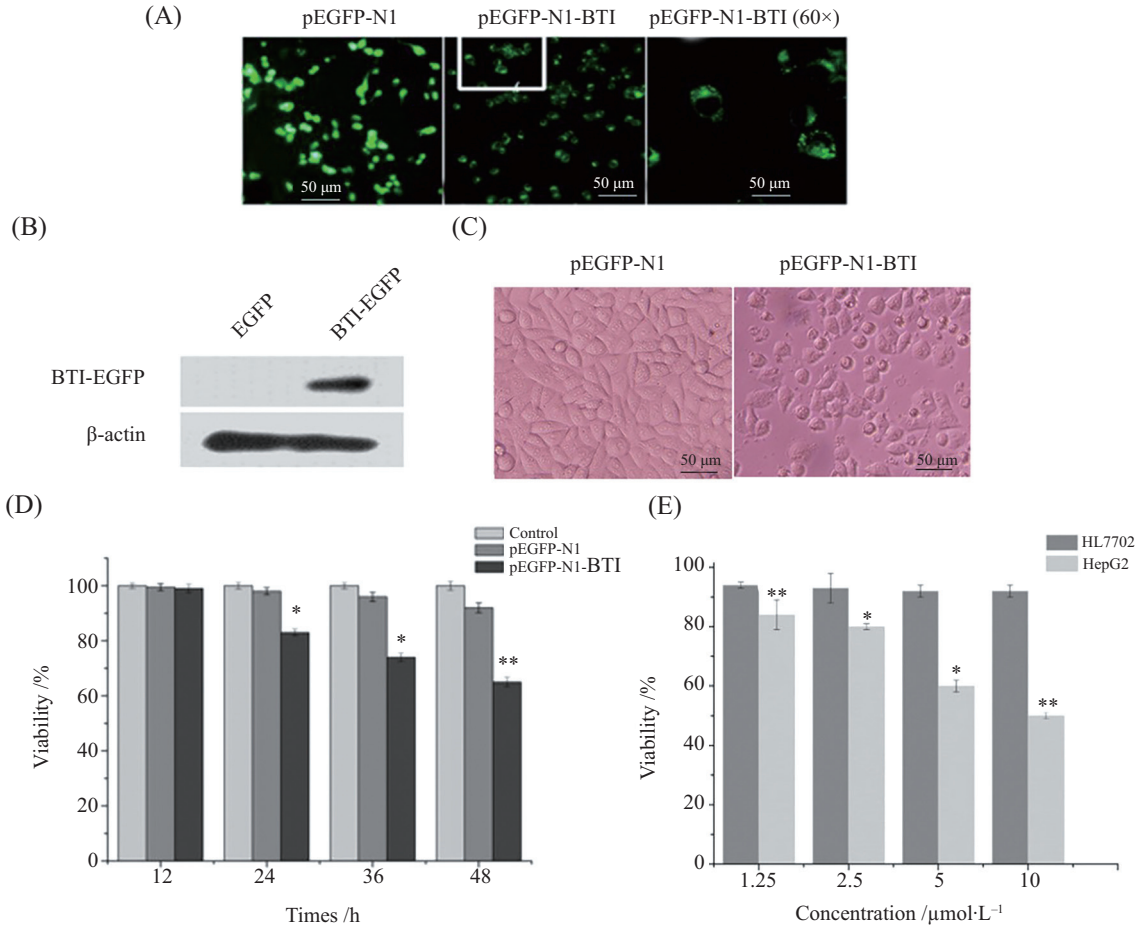

A: 激光共聚焦显微镜观察细胞中绿色荧光蛋白的表达, 图中白框表示放大60×所观察的细胞形态; B: Western blot用于检测BTI在细胞内的表达, β-actin为内参对照; C: 倒置显微镜观察细胞形态; D: MTT法检测细胞活力。*P<0.05, **P <0.01, 与对照组相比较; E: MTT法检测细胞活力。*P<0.05, **P<0.01, 与HL7702细胞组相比较。

A: the laser confocal microscope was used to observe the expression of green fluorescent protein in cells, the white box in the figure represents the cell morphology at a field magnification of 60×; B: BTI expression was detected in HepG2 cells using Western blot. β-actin was used as the internal control; C: cell morphology was observed by the inverted microscope; D: cell viability was measured by MTT assays. *P<0.05, **P<0.01 *vs* control group; E: cell viability was measured by MTT assays. *P<0.05, **P<0.01 *vs* HL7702 cells group.

图1 pEGFP-N1-BTI转染HepG2细胞后细胞活力的变化

Fig.1 The change of viability of HepG2 cells after transfected with pEGFP-N1-BTI

inhibition.

2.2 pEGFP-N1-mediated BTI expression induces cell apoptosis

To define whether pEGFP-N1-mediated BTI expression induced apoptosis of HepG2 cells, we used DAPI to investigate the changes in the cells' nuclei. As clearly shown in Fig.2A, cells transfected with pEGFP-N1 showed homogeneous staining of their nuclei. In contrast, when cells were transfected with pEGFP-N1-BTI for 48 h, apoptotic cells displayed irregular staining of their nuclei because of nuclear fragmentation and chromatin condensation.

Simultaneous staining with Annexin V-FITC and PI distinguished the healthy, early apoptotic, late apoptotic, and dead cells. After transfection with pEGFP-N1 and pEGFP-N1-BTI for 24 and 48 h, apoptosis in hu-

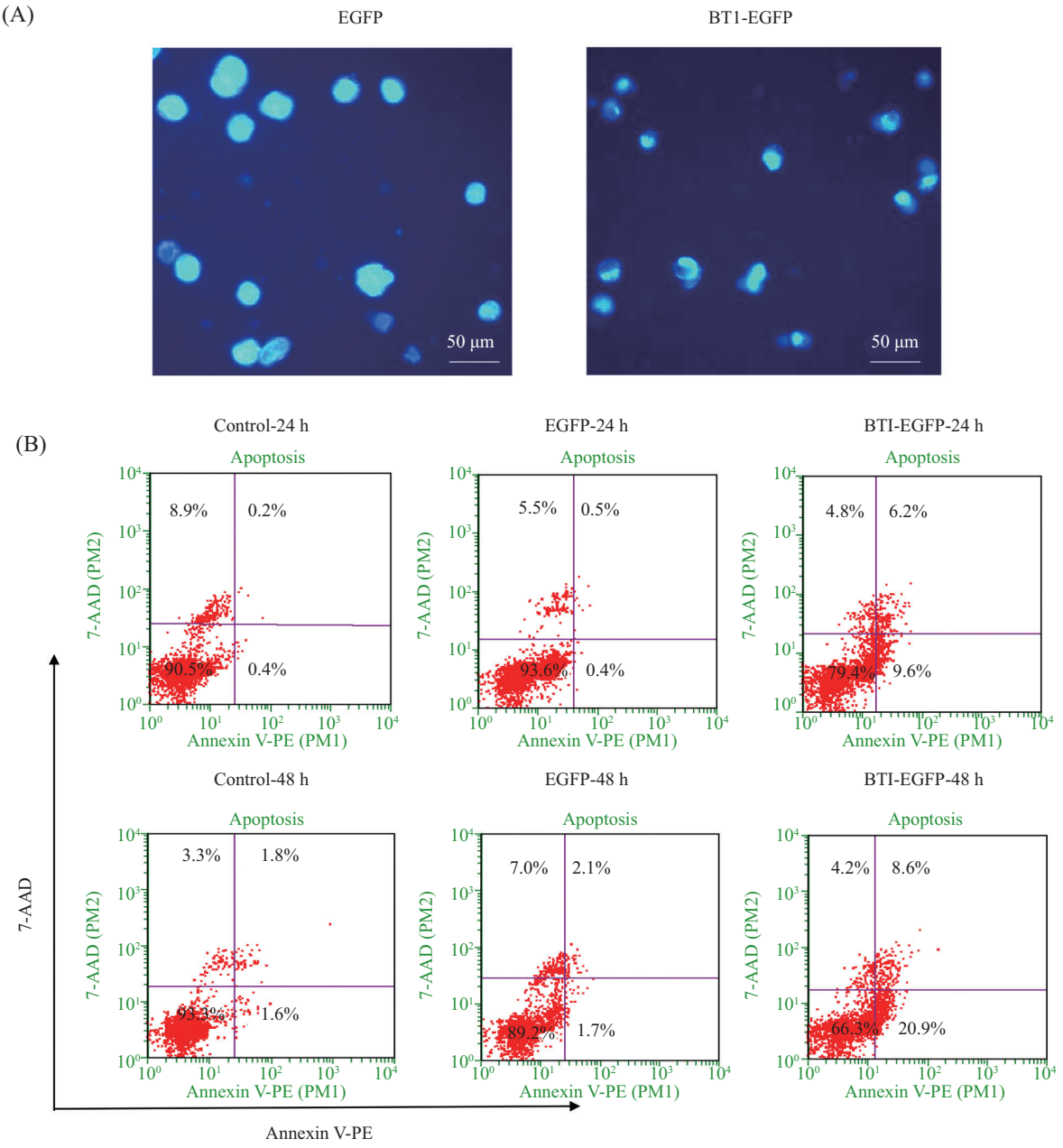

A: 激光共聚焦显微镜观察细胞核的形态学特征; B: 流式细胞仪检测细胞凋亡率。

A: the morphological features of nuclei were evaluated by using a laser confocal microscope; B: apoptosis rates of the cells were analyzed using flow cytometry.

图2 pEGFP-N1-BTI转染对HepG2细胞凋亡的影响

Fig.2 The change of cell apoptosis on HepG2 cells after transfected with pEGFP-N1-BTI

man HepG2 cells was detected by flow cytometry. As shown in Fig.2B, the early and late apoptosis percentages were 0.9 (0.4+0.5)% and 3.8 (1.7+2.1)% when cells were transfected with pEGFP-N1 for 24 and 48 h, respectively. However, the apoptosis percentages were 15.8 (9.6+6.2)% and 29.5 (20.9+8.6)% when the cells were transfected with pEGFP-N1-BTI for 24 and 48 h, respectively. The results indicated that pEGFP-N1-mediated BTI expression induced HepG2 cells apoptosis.

2.3 pEGFP-N1-mediated BTI suppresses the adhesion and migration of HepG2 cells

Before invasion, malignant tumor cells adhere to the ECM (extracellular matrix), and such interaction possibly degrades the ECM. We evaluated the effect of transfected-BTI on HepG2 cells adhesion. As shown in Fig.3A, the D_{570} values were 0.15, 0.34, 0.56, and 0.73 when the cells were transfected with pEGFP-N1 for 1, 2, 3, and 4 h, respectively. The D_{570} values were 0.14, 0.18, 0.23, and 0.28, and the relative cell adhesion rates were 93.3%, 52.9%, 41.1%, and 38.1% when the cells were transfected with pEGFP-N1-BTI for 1, 2, 3, and 4 h, respectively. The data suggested that pEGFP-N1-mediated BTI significantly reduced the cell adhesion rate. We detected the migration ability of pEGFP-N1-BTI transfection via the wound-healing assay. The data displayed that pEGFP-N1-mediated BTI exhibited decreased migration activity at all time points compared with the pEGFP-N1 control (Fig.3B). The widths of the wound were 33.9 and 21.0 μm and migration rate was 38% in the pEGFP-N1 control group. In contrast, the widths of the wound were 35.5 and 32.5 μm and migration rate was 8.45% in the pEGFP-N1-BTI treat-

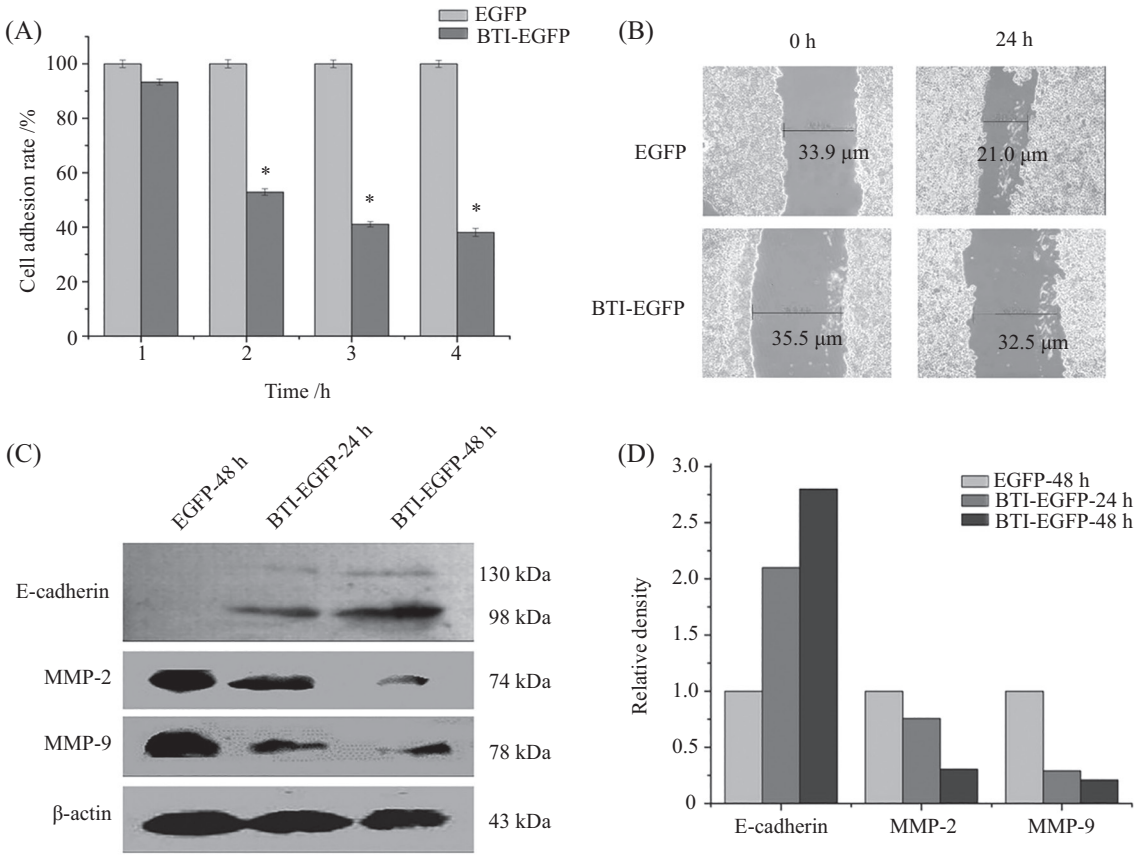

A: HepG2细胞与细胞外基质之间的黏附率检测。*P<0.05, 与EGFP组相比较; B: 伤口愈合擦伤实验检测细胞迁移情况; C: Western blot检测细胞中E-钙黏蛋白, MMP-2和MMP-9的蛋白表达情况, 以β-actin为对照; D: E-cadherin, MMP-2和MMP-9的相对蛋白质水平的分析。

A: the adhesion ratio between HepG2 cells and extracellular matrix. *P<0.05 *vs* EGFP group; B: Wound healing assay was used to evaluate cell migration; C: the protein expression of E-cadherin, MMP-2, and MMP-9 were measured by Western blot. β-actin was used as internal control; D: the relative protein levels of E-cadherin, MMP-2, and MMP-9 were analyzed.

图3 pEGFP-N1-BTI转染HepG2细胞对细胞黏附和迁移的影响

Fig.3 The change of cell adhesion and migration of HepG2 cells after transfected with pEGFP-N1-BTI

ment group. Therefore, pEGFP-N1-mediated BTI expression showed high activity in suppressing cell adhesion and migration.

Adherens junctions are mediated by E-cadherin, and MMPs (matrix metalloproteinases) play a major role in cells migration. To determine whether the E-cadherin and MMPs were involved in the cell adhesion and migration, Western blot analysis was performed. As shown in Fig.3C and Fig.3D, pEGFP-N1-mediated BTI induced E-cadherin protein expression and down-regulated MMP-2 and MMP-9 expressions in HepG2 cells.

2.4 pEGFP-N1-mediated BTI arrests cell cycle

To determine whether pEGFP-N1-mediated BTI's inhibition of cell growth was due to the blockage of cell cycle progression, cell cycle profiles were detected using flow cytometry at 24 and 48 h after transfection. The percentages of cells in the G_1, S, and G_2/M phases are shown in Fig.4A and Fig.4B. The proportion of cells in G_1 phase increased but significantly decreased in G_2/M phase when the cells were transfected with pEGFP-N1-BTI. Thus, pEGFP-N1-mediated BTI expression could arrest HepG2 cell cycle at G_1 period.

To further clarify the mechanism of pEGFP-N1-mediated BTI on HepG2 cell cycle arrest, the expressions of cell cycle key factors were analyzed through Western blot and qRT-PCR. Fig.4C-Fig.4E showed that the pEGFP-N1-mediated BTI up-regulated the expressions of the pro-apoptotic and cycle arrest factors p53, p63, p73, and p21. It down-regulated the cycle-dependent factors CyclinD1, CyclinE1, CDK2, CDK4, and CDK7 by blocking the cell cycle, inhibiting cell

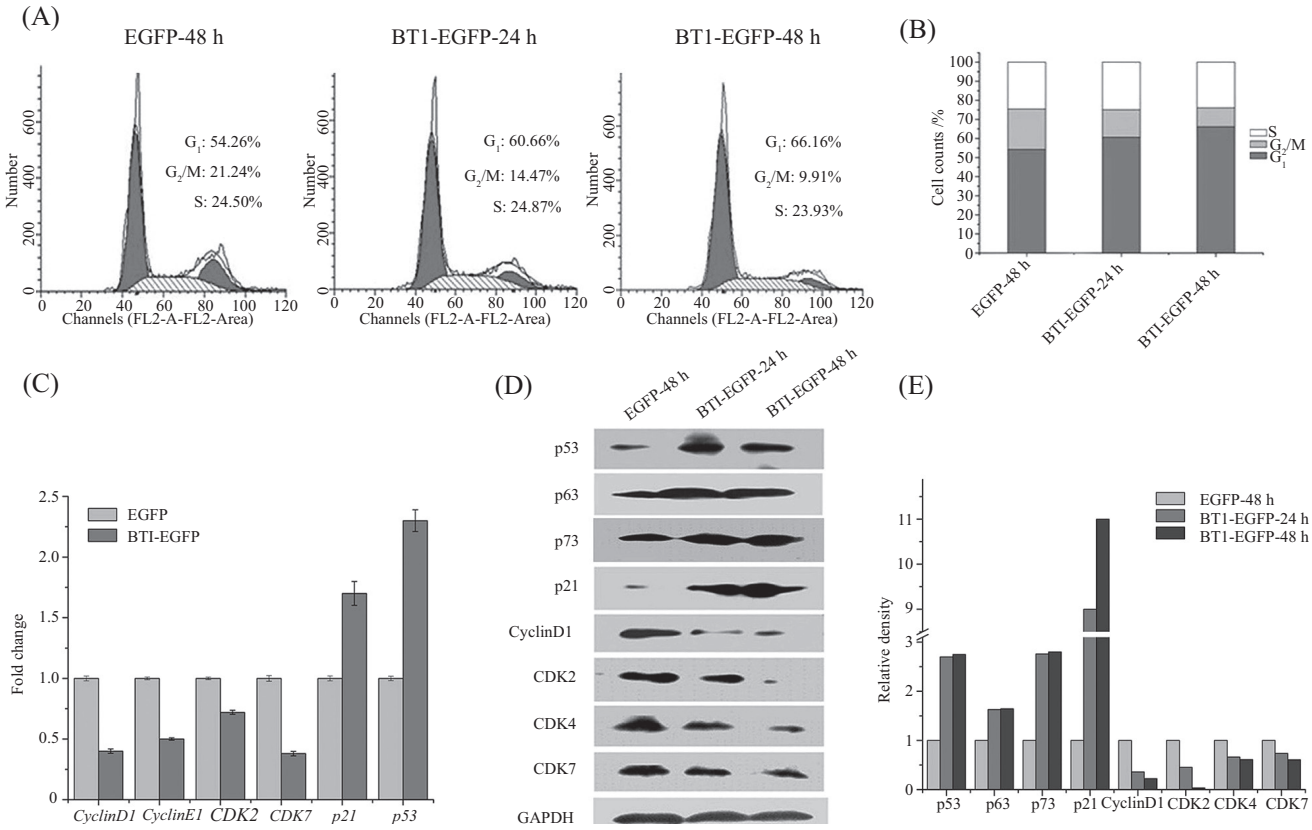

A、B: 流式细胞术检测细胞周期的变化; C: qRT-PCR分析*CyclinD1*、*CyclinE1*、*CDK2*、*CDK7*、*p21*、*p53*的mRNA水平的变化; D: Western blot检测p53、p63、p73、p21、CyclinD1、CDK2、CDK4和CDK7的蛋白的表达, 以GADPH为对照; E: p53、p63、p73、p21、CyclinD1、CDK2、CDK4和CDK7的相对水平分析;

A,B: the change of the cell cycle was detected by flow cytometry; C: the average fold changes on mRNA level of *CyclinD1*, *CyclinE1*, *CDK2*, *CDK7*, *p21*, and *p53* were analyzed by qRT-PCR; D: the protein expression of p53, p63, p73, p21, CyclinD1, CDK2, CDK4, and CDK7 were measured by Western blot; GADPH was used as internal control; E: the relative levels of p53, p63, p73, p21, CyclinD1, CDK2, CDK4, and CDK7 were analyzed.

图4 pEGFP-N1-BTI转染HepG2细胞对细胞周期及周期关键因子的影响

Fig.4 The change of cell cycle and key factors of HepG2 cells after transfected with pEGFP-N1-BTI

proliferation, and inducing cell apoptosis.

3 Discussion

HCC is a problem and a challenge to clinical treatment. More effective treatment methods and strategies are badly needed in the clinic. Tumor gene therapy is restricted by vectors and gene transfecting methods. Clinically, liposome-mediated gene transfer is suitable. Therefore, in the present study, the potential therapeutic effect of pEGFP-N1-mediated BTI against HCC was evaluated *in vitro* and its potential mechanism was explained.

Cell migration and adhesion play a key role in tumor development, wound healing, and immune responses. Extracellular Ca^{2+} promotes cell differentiation in epidermal keratinocytes by raising intracellular free Ca^{2+} levels and initiating intercellular adhesion[9]. E-cadherin has played a signaling role complementary to its adhesion capacity and is involved in multiple processes, including the establishment of tissue limits and proliferation, as well as cell migration. The occurrence, development, invasion, and metastasis of malignant tumors are often accompanied by changes in the expression of ECM and its cell surface receptors. The degradation of ECM by MMPs is one of the key links of tumor cell invasion and metastasis. Various malignant tumors are accompanied by increased secretion levels and activities of MMPs[10]. MMPs are a family of structurally and functionally related endopeptidases that can degrade the collagenous and non-collagenous ECM components. Among MMPs, MMP-2 and MMP-9 play important roles in malignant tumors development[11]. In the present study, the data indicated that pEGFP-N1-mediated BTI expression in HepG2 cells showed high activity in inhibiting cell proliferation, adhesion, and migration by inducing E-cadherin expression and decreasing MMP-2 and MMP-9 expressions.

An out-of-control cell cycle is an important cause of carcinogenesis. In cell cycle regulation, the most important regulation point is between the G_1 and S phases. If this regulatory point is abnormal, then abnormal cell proliferation will lead to tumor formation. Cell cycle regulation is controlled by a regulatory subunit (the Cyclin family) and a catalytic component designated as CDK (Cyclin-dependent kinase)[12]. CyclinD1 is a proto-oncogene involved in the occurrence and development of tumors and is the most closely related to tumor proliferation among the cyclins. Overexpression of CyclinD1 can lead to the dysregulation of the control points of tumor cells from G_1 to S phase, thereby shortening the G_1 phase. Inhibiting the CyclinD1 expression can inhibit the progression of cells to the S phase[13]. CyclinE1 is an oncogene often being regarded as an S phase marker, and its overexpression is associated with tumor invasion. CyclinE1 is a molecular-biological marker for cancer diagnosis and prognosis monitoring[14].

p21 is a very common cyclin-dependent kinase inhibitor CDKI that can combine with a variety of Cyclin-CDKs to inhibit cell proliferation. p21 can enhance DNA repair and can be used to eliminate tumor occurrence caused by the accumulation of DNA damage. p21 overexpression can significantly inhibit the rapid proliferation of tumor cells, and it is a key participant in tumor gene therapy[15]. CDK4 is a cell cycle-dependent kinase that serves as a key regulator of cell cycle G_1-S phase. CDK4 activation leads to the increased degradation of p21, which in turn facilitates CDK2 activation[16].

p53 is a tumor suppressor gene that can inhibit tumor cell proliferation and induce apoptosis. p53 is reportedly closely related to HCC occurrence and development[17]. p63 and p73, the same as p53, can transactivate *PUMA* and *Bax* genes, thereby inducing tumor cell apoptosis. Kim et al[18] find that p53 is important for HCC cells growth and that p53-regulated PUMA reduces mitochondrial pyruvate uptake and increases glycolysis in HCC. Thus, researchers possibly need to be careful when designing cancer treatment strategies that activate p53. p63 and p73 can control cell cycle and cell death with mechanisms often similar to those initially ascribed only to p53. We confirmed that pEGFP-N1-mediated BTI arrested HepG2 cells cycle in the G_1 phase by involving p53 and p53 family up-

regulation, CyclinD1, CyclinE1, and cyclin-dependent kinases down-regulation.

The present study demonstrated that pEGFP-N1-mediated BTI induced HepG2 cells apoptosis and G_1 phase arrest through the activation of p53, p63, p73, and p21 and by decreasing CyclinD1, CyclinE1, CDK2, CDK4, and CDK7 expressions. pEGFP-N1-mediated BTI could promote E-cadherin protein expression and decrease MMP-2 and MMP-9 expressions. Moreover, cell adhesion was reduced, and cell proliferation and migration were significantly inhibited. The findings presented in this study are essential for the further exploration of the BTI gene therapy of HCC.

References

[1] KEATING G M. Sorafenib: a review in hepatocellular carcinoma [J]. Target Oncol, 2017, 12: 243-53.

[2] KUDO M, FINN R S, QIN S K, et al. Lenvatinib versus sorafenib in first-line treatment of patients with unresectable hepatocellular carcinoma: a randomised phase 3 non-inferiority trial [J]. Lancet, 2018, 391(10126): 1163-73.

[3] INOUE K, TAKANO H, YANAGISAWA R, et al. Protective role of urinary trypsin inhibitor in acute lung injury induced by lipopolysaccharide [J]. Exp Biol Med, 2005, 230: 281-7.

[4] BIJINA B, CHELLAPPAN S, KRISHNA J G, et al. Protease inhibitor from Moringa oleifera with potential for use as therapeutic drug and as seafood preservative [J]. Saudi J Biol Sci, 2011, 18(3): 273-81.

[5] ARMSTRONG W B, TAYLOR T H, KENNEDY A R, et al. Bowman-birk inhibitor concentrate and Oral Leukoplakia: a randomized phase IIb trial [J]. Cancer Prev Res, 2013, 6(5): 410-8.

[6] PARK S S, OHBA H. Suppressive activity of protease inhibitors from buckwheat seeds against human T-acute lymphoblastic leukemia cell lines [J]. Appl Biochem Biotech, 2004, 117: 65-74.

[7] LI Y Y, ZHANG Z, WANG Z H, et al. rBTI induces apoptosis in human solid tumor cell lines by loss in mitochondrial transmembrane potential and caspase activation [J]. Toxicol Lett, 2009, 189: 166-75.

[8] LI Y Y, WU Y Z, CUI X D, et al. NFκB/p65 activation is involved in regulation of rBTI-induced glucocorticoid receptor expression in MCF-7 cell lines [J]. J Funct Foods, 2015, 15: 376-88.

[9] GONZALEZ S, IBANEZ E, SANTALO J. Influence of E-cadherin-mediated cell adhesion on mouse embryonic stem cells derivation from isolated blastomeres [J]. Stem Cell Rev Rep, 2011, 7: 494-505.

[10] XIE Z J, BIKLE D D. The recruitment of phosphatidylinositol 3-kinase to the E-cadherin-catenin complex at the plasma membrane is required for calcium-induced phospholipase C-1 activation and human keratinocyte differentiation [J]. J Biol Chem, 2007, 282: 8695-703.

[11] LI W, LI N, SONG D, et al. Metformin inhibits endothelial progenitor cell migration by decreasing matrix metalloproteinases, MMP-2 and MMP-9, via the AMPK/mTOR/autophagy pathway [J]. Int J Mol Med, 2017, 39: 1262-8.

[12] INGHAM M, SCHWARTZ G K. Cell-cycle therapeutics come of age [J]. J Clin Oncol, 2017, 35: 2949-59.

[13] GANUZA M, SAIZ-LADERA C, CANAMERO M, et al. Genetic inactivation of Cdk7 leads to cell cycle arrest and induces premature aging due to adult stem cell exhaustion [J]. Embo J, 2012, 31: 2498-510.

[14] GUO R, OVERMAN M, CHATTERJEE D, et al. Aberrant expression of p53, p21, cyclin D1, and Bcl2 and their clinicopathological correlation in ampullary adenocarcinoma [J]. Hum Pathol, 2014, 45: 1015-23.

[15] BENDRIS N, LEMMERS B, BLANCHARD J M. Cell cycle, cytoskeleton dynamics and beyond: the many functions of cyclins and CDK inhibitors [J]. Cell Cycle, 2015, 14(12): 1786-98.

[16] BISTEAU X, PATERNOT S, COLLEONI B, et al. CDK4 T172 phosphorylation is central in a CDK7-dependent bidirectional CDK4/CDK2 interplay mediated by p21 phosphorylation at the restriction point [J]. PLoS Genet, 2013, 9: e1003546.

[17] KANG H J, ROSENWAKS Z. p53 and reproduction [J]. Fertil Steril, 2018, 109(1): 39-43.

[18] KIM J, YU L, CHEN W, et al. Wild-type p53 promotes cancer metabolic switch by inducing PUMA-dependent suppression of oxidative phosphorylation [J]. Cancer Cell, 2019, 35: 191-203.